Journal of Glaciology



Letter

Cite this article: Greve R (2025) On non-dimensional forms of basal sliding laws and flow laws for ice-sheet and glacier modelling. *Journal of Glaciology* **71**, e123, 1–6. https://doi.org/10.1017/jog.2025.10100

Received: 26 June 2025 Revised: 22 October 2025 Accepted: 23 October 2025

Keywords:

glacier flow; glacier modelling; ice dynamics; ice-sheet modelling

Email: greve@lowtem.hokudai.ac.jp

On non-dimensional forms of basal sliding laws and flow laws for ice-sheet and glacier modelling

Ralf Greve 📵

Institute of Low Temperature Science, Hokkaido University, Sapporo, Japan and Arctic Research Center, Hokkaido University, Sapporo, Japan

Abstract

Ice sheets and glaciers flow through basal sliding and internal deformation, each governed by physical laws commonly expressed as power-law relations. These formulations include coefficients—the sliding coefficient and rate factor—whose values and units depend on the respective exponents. This dependency complicates the systematic exploration of parameter space, especially in ensemble simulations. To address this, we propose dimensionless formulations of both sliding and flow laws, in which the coefficients are of order unity and decoupled from the exponents. This separation simplifies sensitivity studies and parameter variations. The dimensionless laws are straightforward to implement in existing models; we demonstrate this with the SICOPOLIS icesheet model using three test simulations in an idealized set-up. These simulations illustrate that independent variation of exponents and coefficients is feasible and practical, supporting the use of dimensionless laws in efforts to better constrain ice dynamics in past and future climate scenarios.

1. Introduction

Ice sheets and glaciers flow due to two different processes, namely basal sliding and internal deformation. Basal sliding describes the sliding of glacier ice on the underlying substrate, which can be either hard bedrock or a deformable sediment layer between ice and bedrock. Internal deformation is governed by the non-linear viscous properties of "hot" polycrystalline ice (that is, with a homologous temperature $T/T_{\rm m}$ near unity, where T is the absolute temperature and $T_{\rm m}$ the pressure melting point).

In a dynamic/thermodynamic ice sheet or glacier model, both processes must be included. Basal sliding, which in reality is a complex process that depends on a multitude of factors such as the basal temperature, roughness of the bedrock, softness of the subglacial sediment layer (if existing) and hydrological conditions, is usually parameterized by a sliding law that relates the sliding velocity to the basal stresses. Internal deformation can be modelled by a non-linear viscous flow law that describes the relation between the macroscopic deformation (strain rate) and internal stresses (e.g., Hooke, 2005; Greve and Blatter, 2009; Cuffey and Paterson, 2010).

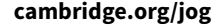
Popular forms for such relations are the Weertman–Budd sliding law and the Nye–Glen flow law (see below for references). They have in common that they are expressed as power laws with some exponents, of which the optimal values are debated, and contain a factor to close the respective equation. This factor, the "sliding coefficient" in case of the sliding law and the "rate factor" in case of the flow law, may contain remaining dependencies, such as on the temperature. In a dimensional formulation, the units and numerical values of these factors depend strongly on the choice of the exponents, which makes it cumbersome to vary the exponents over their potential range of values, for instance, within an ensemble of simulations for a given scenario. To overcome this obstacle, we propose fully or partly dimensionless versions of the sliding and flow laws, which have in common that the respective factor is dimensionless and generally of order unity. These formulations decouple the value of the exponents from the value of the factor, so that the factors and exponents can be varied independently. We demonstrate this useful feature by some simple simulations with the ice-sheet model SICOPOLIS (SImulation COde for POLythermal Ice Sheets; SICOPOLIS Authors, 2025).

2. Basal sliding laws

Basal sliding laws (aka basal friction laws) relate the shear stress (drag) at the base of an ice sheet or glacier, τ_b , to the basal normal stress, N_b and the basal sliding velocity, v_b . In a general, implicit form, a basal sliding law can be expressed as

$$f(\nu_{\mathbf{b}}, \tau_{\mathbf{b}}, N_{\mathbf{b}}) = 0, \tag{1}$$

© The Author(s), 2025. Published by Cambridge University Press on behalf of International Glaciological Society. This is an Open Access article, distributed under the terms of the Creative Commons Attribution licence (http://creativecommons.org/licenses/by/4.0), which permits unrestricted re-use, distribution and reproduction, provided the original article is properly cited.





2 Ralf Greve

where f is a function unspecified at this stage. The list of variables is not necessarily exhaustive as further dependencies, for instance on basal temperature or the presence of basal water, may be included. Note that, in the presence of subglacial water, the basal normal stress is often understood as the difference between the ice overburden stress, $N_{\rm b,i}$, and the basal water pressure, $p_{\rm b,w}$,

$$N_{\rm b} = N_{\rm b.i} - p_{\rm b.w},$$
 (2)

and then called the reduced normal stress or, alternatively, the effective pressure.

A popular form of a basal sliding law is the Weertman–Budd sliding law, which results when assuming an explicit form of Eq. (1) solved for v_b , with power-law dependencies on τ_b and N_b :

$$\nu_{\rm b} = C_{\rm b} \frac{\tau_{\rm b}^p}{N_{\rm b}^q},\tag{3}$$

where C_b is the sliding coefficient and (p,q) are the non-negative sliding exponents (Weertman, 1957; Budd and others, 1979, 1984; Budd and Jenssen, 1987). Alternatively, Eq. (3) can be solved for the shear stress,

$$\tau_{\rm b} = C_{\rm b}^{\star} v_{\rm b}^{1/p} N_{\rm b}^{q/p}, \quad \text{with } C_{\rm b}^{\star} = C_{\rm b}^{-1/p},$$
 (4)

where C_b^{\star} is the basal friction coefficient. For the case q=0, that is, ignoring the dependence on the normal stress N_b , the above forms are often referred to as the Weertman sliding law.

In principle, $v_{\rm b}$ and $\tau_{\rm b}$ are vector quantities. For simplicity, we formulate the sliding laws only with the respective magnitudes. However, to interpret the results correctly, it must be kept in mind that $v_{\rm b}$ and $\tau_{\rm b}$ are anti-parallel to each other due to the nature of friction.

Let us now non-dimensionalize the sliding law (3) by introducing scales (typical values) for the relevant quantities (e.g., Hutter and Jöhnk, 2004). We consider a situation near the edge of an ice sheet where basal sliding is most relevant:

$$[H] = 1 \text{ km} \quad \text{(typical thickness)}, \tag{5a}$$

$$\varepsilon = 10^{-2}$$
 (typical surface slope), (5b)

$$[N_b] = \rho g[H] = 10^7 \,\text{Pa}$$
 (typical normal stress), (5c)

$$[\tau_b] = \varepsilon [N_b] = 10^5 \,\text{Pa}$$
 (typical shear stress), (5d)

$$[v_b] = 100 \,\mathrm{m}\,\mathrm{a}^{-1}$$
 (typical sliding velocity), (5e)

where we have used approximate values $\rho \approx 10^3 \, \mathrm{kg \, m^{-3}}$ for the ice density and $g \approx 10 \, \mathrm{m \, s^{-2}}$ for the acceleration due to gravity, which is sufficiently accurate for the sake of a scaling analysis. This scaling is consistent with the linear sliding law $[C_b = 10^{-3} \, \mathrm{m \, a^{-1} \, Pa^{-1}}, \, (p,q) = (1,0)]$ used for the EISMINT Phase 2 Simplified Geometry Experiments (Payne and others, 2000):

$$\underbrace{100\,\mathrm{m}\,\mathrm{a}^{-1}}_{\nu_{\mathrm{b}}} = \underbrace{10^{-3}\,\mathrm{m}\,\mathrm{a}^{-1}\,\mathrm{Pa}^{-1}}_{C_{\mathrm{b}}} \times \underbrace{10^{5}\,\mathrm{Pa}}_{\tau_{\mathrm{b}}}. \tag{6}$$

An appropriate choice for the scale of the sliding coefficient results from Eq. (3) as

$$[C_{\rm b}] = \frac{[\nu_{\rm b}][N_{\rm b}]^q}{[\tau_{\rm b}]^p}. (7)$$

We now use the above scales to introduce dimensionless quantities as follows:

$$v_{\mathbf{b}} = [v_{\mathbf{b}}] \, \tilde{v}_{\mathbf{b}},\tag{8a}$$

$$\tau_{\mathbf{b}} = [\tau_{\mathbf{b}}] \, \tilde{\tau}_{\mathbf{b}},\tag{8b}$$

$$N_{\rm b} = [N_{\rm b}] \, \tilde{N}_{\rm b},\tag{8c}$$

$$C_{\rm b} = [C_{\rm b}] \, \tilde{C}_{\rm b},\tag{8d}$$

where the quantities marked by the tilde symbol are the nondimensional basal sliding velocity, shear stress, normal stress and sliding coefficient, respectively. Inserting Eq. (8) in the sliding law (3) yields its fully non-dimensional form,

$$\tilde{v}_{b} = \tilde{C}_{b} \frac{\tilde{\tau}_{b}^{p}}{\tilde{N}_{b}^{q}},\tag{9}$$

in which all quantities are supposed to be of order unity.

A dimensional form of Eq. (3) can be kept by only making use of the scaling (8d) of the sliding coefficient,

$$\nu_{\rm b} = [C_{\rm b}] \, \tilde{C}_{\rm b} \frac{\tau_{\rm b}^p}{N_{\rm b}^q},\tag{10}$$

which has the advantage that its implementation in an existing model based on dimensional quantities requires only minimal adaptations.

In order to obtain the fully or partly dimensionless counterparts of Eq. (4), we note the scaling and non-dimensionalization of the friction coefficient C_b^* :

$$C_{\rm b}^{\star} = [C_{\rm b}^{\star}] \, \tilde{C}_{\rm b}^{\star}, \quad \text{with } [C_{\rm b}^{\star}] = [C_{\rm b}]^{-1/p} = \frac{[\tau_{\rm b}]}{[\nu_{\rm b}]^{1/p} [N_{\rm b}]^{q/p}}.$$
 (11)

The fully non-dimensional form of Eq. (4) results then as

$$\tilde{\tau}_{\mathbf{b}} = \tilde{C}_{\mathbf{b}}^{\star} \, \tilde{v}_{\mathbf{b}}^{1/p} \tilde{N}_{\mathbf{b}}^{q/p}, \tag{12}$$

and the dimensional form in which only the scaling (11) of the friction coefficient is used reads

$$\tau_{\rm b} = [C_{\rm b}^{\star}] \, \tilde{C}_{\rm b}^{\star} \, \nu_{\rm b}^{1/p} N_{\rm b}^{q/p}. \tag{13}$$

Why do we promote using Eqs. (10) or (13) instead of Eqs. (3) or (4) in an ice sheet or glacier model? In Table 1 we have compiled some parameter combinations that were used along with Weertman or Weertman-Budd sliding laws in the literature. The impossibility of comparing the various dimensional sliding coefficients C_b for different exponents (p,q) becomes immediately evident. They do not even have a common unit, and the respective numerical value tells nothing about the actual strength of basal sliding. In the second case, (p,q) = (1,2), the numerical value of C_b is greater than 10⁹; however, the small dimensionless value means that it produces only very little basal sliding ($\tilde{C}_b \approx 0.04$). By contrast, in the third case, (p,q) = (3,0), the numerical value of C_b is merely 10^{-12} ; however, it corresponds to pronounced basal sliding ($\tilde{C}_{\rm b}=10$). The dimensionless sliding coefficients $\tilde{C}_{\rm b}$ give a much better idea about what the respective value means physically, and allow comparing values across different sliding laws.

To further strengthen our point, suppose that we wish to test a sliding law with a new set of exponents, for instance (p,q)=(3,1.5). Working with the dimensional sliding coefficient $C_{\rm b}$, we

Journal of Glaciology 3

Table 1. Sliding exponents (p,q), dimensional sliding coefficients $C_{\rm b}$, scales $[C_{\rm b}]$ and dimensionless sliding coefficients $\tilde{C}_{\rm b}$ for several Weertman (q=0) or Weertman–Budd (q>0) sliding laws used in the literature

(p,q)	C_{b}	$[C_{\rm b}]$	$ ilde{C}_{ m b}$	Reference
(1,0)	$10^{-3}\mathrm{ma^{-1}Pa^{-1}}$	$10^{-3} \mathrm{m}\mathrm{a}^{-1}\mathrm{Pa}^{-1}$	1	Payne and others 2000
(1, 2)	$3.985 \times 10^9 \mathrm{ma^{-1}Pa}$	$10^{11}\mathrm{ma^{-1}Pa}$	0.03985	Budd and others 1984†
(3, 0)	$10^{-12}\mathrm{ma^{-1}Pa^{-3}}$	$10^{-13}\mathrm{ma^{-1}Pa^{-3}}$	10	Cornford and others 2020
(3, 1)	$\begin{array}{l} 1.607 \; \times \\ 10^{-6} \mathrm{m} \mathrm{a}^{-1} \mathrm{Pa}^{-2} \end{array}$	$10^{-6}\mathrm{m}\mathrm{a}^{-1}\mathrm{Pa}^{-2}$	1.607	Saito and others 2016†
(3, 2)	$6.72\mathrm{ma^{-1}Pa^{-1}}$	$10 \mathrm{m a^{-1} Pa^{-1}}$	0.672	Rückamp and others 2019

^{†:} Rather than using the normal stress $N_{\rm b}$, these sliding laws were formulated with the pressure head $Z=N_{\rm b}/(\rho g)$. We converted the sliding coefficients given in these studies accordingly, using $\rho=910\,{\rm kg\,m^{-3}}$ and $g=9.81\,{\rm m\,s^{-2}}$.

would not have any idea which order of magnitude may be suited for its numerical value, and which range of values mean strong or weak sliding. However, if the dimensionless sliding coefficient \tilde{C}_b is used, we can immediately start with an initial guess $\tilde{C}_b=1$ and, from there on, refine the sliding law by, e.g., tuning to observed flow speeds. According to the scaling (7), (8d), the dimensional equivalent of $\tilde{C}_b=1$ would be $C_b=[C_b]=10^{-2.5}\,\mathrm{m\,a^{-1}\,Pa^{-1.5}}=3.162\times10^{-3}\,\mathrm{m\,a^{-1}\,Pa^{-1.5}}.$

We have only discussed cases with a constant sliding parameter; however, the non-dimensionalization method is of course not limited to this. It can also be applied to a spatially variable sliding coefficient, which may arise from an inversion procedure (e.g., Morlighem and others, 2013). Alternative sliding laws, such as the Coulomb-limited rules discussed by Cornford and others 2020, allow similar non-dimensionalization, although we refrain from working out the details here.

3. Flow laws

A similar problem of units and hugely varying numerical values arises for the flow law of polycrystalline ice. It is a viscous flow law that relates the strain-rate (stretching) tensor d_{ij} to the stress deviator $t_{ii}^{\rm D}$. The strain-rate tensor is defined as

$$d_{ij} = \frac{1}{2} \left(\frac{\partial v_i}{\partial x_j} + \frac{\partial v_j}{\partial x_i} \right) \quad (i, j = 1, 2, 3), \tag{14}$$

where x_i denotes the Cartesian coordinates ($x_1 = x, x_2 = y, x_3 = z$), and v_i is the velocity vector. The stress deviator is the traceless part of the full stress tensor t_{ij} ,

$$t_{ii} = -p \,\delta_{ii} + t_{ii}^{\mathrm{D}},\tag{15}$$

where $p=-t_{ii}/3$ is the pressure (we assume the Einstein summation convention: summation over the twice-appearing index i implied, thus t_{ii} is the trace of the stress tensor), and δ_{ij} is the Kronecker delta symbol, in other words, the unit tensor in index notation

For the flow law, usually collinearity between the symmetric tensors d_{ij} and t_{ij}^{D} is assumed. We note the form given by Greve and Blatter 2009,

$$d_{ii} = Af(\tau_e) t_{ii}^{\mathrm{D}}, \tag{16}$$

where A is the rate factor, $\tau_{\rm e} = [(t_{ij}^{\rm D} t_{ij}^{\rm D})/2]^{1/2}$ the effective stress (summation over both i and j implied), and $f(\tau_{\rm e})$ is the creep function. The rate factor depends on the temperature relative to the

pressure melting point, T', via an Arrhenius law (e.g., Cuffey and Paterson, 2010), but it is sometimes chosen as a constant parameter for simplicity. In the Nye–Glen flow law (Glen, 1955; Nye, 1957), the creep function is expressed as a power law,

$$f(\tau_e) = \tau_e^{n-1},\tag{17}$$

so that

$$d_{ii} = A\tau_e^{n-1} t_{ii}^{\mathrm{D}}, \tag{18}$$

where n is the stress exponent. A value of n=1 would correspond to a Newtonian fluid; however, the deformability of ice differs markedly from that behaviour, and the value is frequently chosen as n=3, or within the range from 1.5 to 4.2 (Cuffey and Paterson, 2010) (while recent evidence from laboratory experiments actually supports n=1 for temperate ice; Schohn and others, 2025).

The Nye-Glen flow law (18) can also be inverted for the stress deviator,

$$t_{ij}^{\rm D} = A^* d_{\rm e}^{-(1-1/n)} d_{ij}, \text{ with } A^* = A^{-1/n},$$
 (19)

where A^* is the associated rate factor and $d_e = [(d_{ij}d_{ij})/2]^{1/2}$ the effective strain rate (e.g., Greve and Blatter, 2009).

Similar to the procedure in Sect. 2, we now introduce scales (typical values) for the relevant quantities, considered suitable for areas where rather large deformations take place:

$$[\tau] = 10^5 \,\mathrm{Pa}$$
 (typical deviatoric stress), (20a)

$$[d] = 2.5 \times 10^{-2} \,\mathrm{a}^{-1}$$
 (typical strain rate), (20b)

where the scale $[\tau]$ is deemed appropriate for both t_0^D and τ_e . Using Eq. (18) entails the choice for the scale of the rate factor:

$$[A] = \frac{[d]}{[\tau]^n}. (21)$$

We introduce the dimensionless quantities

$$t_{ij}^{\mathrm{D}} = [\tau] \tilde{t}_{ij}^{\mathrm{D}}, \tag{22a}$$

$$\tau_e = [\tau] \, \tilde{\tau}_e, \tag{22b}$$

$$d_{ij} = [d] \tilde{d}_{ij}, \qquad (22c)$$

$$A = [A] \tilde{A}, \tag{22d}$$

where the quantities marked by the tilde symbol are the nondimensional components of the stress deviator, effective stress, components of the strain-rate tensor and rate factor, respectively.

For n=3, Eq. (21) yields $[A]=2.5\times 10^{-17}\,\mathrm{a}^{-1}\,\mathrm{Pa}^{-3}=7.922\times 10^{-25}\,\mathrm{s}^{-1}\,\mathrm{Pa}^{-3}$. This value is close to the recommendation by Cuffey and Paterson 2010 for $T'=-6^{\circ}\mathrm{C}$, which demonstrates the validity of our scaling.

We obtain the fully non-dimensional form of the flow law (18)

$$\tilde{d}_{ij} = \tilde{A} \, \tilde{\tau}_{e}^{n-1} \, \tilde{t}_{ij}^{D}, \tag{23}$$

(all quantities supposed to be of order unity). A form with only *A* scaled results if we only apply the scaling (22d):

$$d_{ii} = [A]\tilde{A}\,\tau_e^{n-1}\,t_{ii}^{\mathrm{D}}.\tag{24}$$

Analogous to the sliding law (10), this form can be implemented in a model based on dimensional quantities with only minimal changes. 4 Ralf Greve

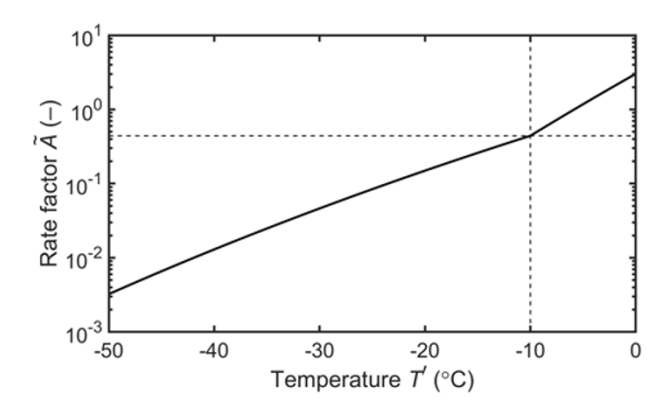


Figure 1. Dimensionless rate factor \tilde{A} as a function of the temperature relative to pressure melting T', following the recommendation by Cuffey and Paterson 2010: Arrhenius law with activation energies $Q=60\,\mathrm{kJ\,mol^{-1}}$ for $T'\leqslant-10^\circ\mathrm{C}$, $Q=115\,\mathrm{kJ\,mol^{-1}}$ for $T'\geqslant-10^\circ\mathrm{C}$, $A=3.5\times10^{-25}\,\mathrm{s^{-1}\,Pa^{-3}}$ for $T'=-10^\circ\mathrm{C}$ and n=3.

To obtain the fully or partly dimensionless versions of Eq. (19), we note the scaling and non-dimensionalization of the associated rate factor A^* ,

$$A^* = [A^*] \tilde{A}^*, \text{ with } [A^*] = [A]^{-1/n} = \frac{[\tau]}{[d]^{1/n}},$$
 (25)

and for the effective strain rate, the scale (20b) is used,

$$d_{\rm e} = [d] \, \tilde{d}_{\rm e}. \tag{26}$$

The fully non-dimensional form of Eq. (19) is then

$$\tilde{t}_{ij}^{\mathrm{D}} = \tilde{A}^{\star} \, \tilde{d}_{\mathrm{e}}^{-(1-1/n)} \, \tilde{d}_{ij}, \tag{27}$$

and the form with only A^* scaled reads

$$t_{ij}^{\rm D} = [A^{\star}]\tilde{A}^{\star} d_{\rm e}^{-(1-1/n)} d_{ij}.$$
 (28)

Figure 1 shows the temperature-dependent rate factor following the recommendation by Cuffey and Paterson 2010, non-dimensionalized with the scaling (21), (22d). However, while the original recommendation in dimensional form is valid only for n=3, this dimensionless form can be used for any value of the stress exponent n. It is therefore much more flexible.

Consider the case n=4, which has recently been discussed by, e.g., Bons and others (2018); Millstein and others (2022); Getraer and Morlighem (2025). The unit of the rate factor A must then be a^{-1} Pa $^{-4}$, but what about suitable numerical values? When using the dimensionless formulation promoted here, there is no problem; $\mathcal{O}(1)$ values will be suitable for the high-temperature regime (i.e., temperatures close to pressure melting) just like for any other value of n, and we can use the function shown in Figure 1 as a starting point. According to Eq. (21), the scale for A changes to $[A] = 2.5 \times 10^{-22}$ a $^{-1}$ Pa $^{-3}$ for n=3), so that $\tilde{A}=1$ corresponds to $A=2.5\times 10^{-22}$ a $^{-1}$ Pa $^{-4}$.

The non-dimensionalization method is not limited to the Nye-Glen flow law discussed above. A straightforward extension is for its regularized version with the creep function $f(\tau_{\rm e}) = \tau_{\rm e}^{n-1} + \tau_{\rm 0}^{n-1}$, where $\tau_{\rm 0}$ is the residual stress, a small constant introduced to avoid the infinite-viscosity limit for vanishing stresses or strain rates (Greve and Blatter, 2009). For this flow law, Eqs. (20)–(22) remain applicable. However, it cannot be analytically inverted for the stress deviator; this is only possible by numerically solving

Table 2. Set-up of the experiments H1, H2 and H3: Sliding exponents (p,q), dimensionless sliding coefficient $\tilde{C}_{\rm b}$, stress exponent n, dimensionless rate factor \tilde{A} ($\tilde{A}_{\rm CP10}$ denotes the non-dimensionalized rate factor by Cuffey and Paterson 2010 as shown in Figure 1). Note that $\tilde{C}_{\rm b}$ and \tilde{A} are the same for all experiments

Experiment	(p,q)	$ ilde{C}_{ m b}$	n	$ ilde{A}$
H1	(1,0)	1	3	$\tilde{A}_{ ext{CP10}}$
H2	(3, 2)	1	3	$ ilde{A}_{ ext{CP10}}$
H3	(1,0)	1	4	$ ilde{A}_{ ext{CP10}}$

an implicit equation. Further flow laws shall not be considered here.

4. Tests with the ice-sheet model SICOPOLIS

Replacing the previously implemented, dimensional versions, the Weertman–Budd basal sliding law formulated with the dimensionless sliding coefficient, Eqs. (10) and (13), and the Nye–Glen flow law formulated with the dimensionless rate factor, Eqs. (24) and (28), have both been introduced in the ice-sheet model SICOPOLIS v25 (SICOPOLIS Authors, 2025), revision 3e7e6c939 of 17 June 2025. Details of the implementation can be found in Sect. 6 ("Modelling choices") of the ReadTheDocs manual at https://sicopolis.readthedocs.io/ (last access: 26 June 2025).

We briefly demonstrate the benefit of the new formulation by considering experiment H of the EISMINT Phase 2 Simplified Geometry Experiments (Payne and others, 2000). The original setup of this experiment uses the Weertman sliding law with (p,q)=(1,0) and $C_{\rm b}=10^{-3}$ m a⁻¹ Pa⁻¹, only applied for a temperate base, while no-slip conditions are assumed for a cold base. The value of the sliding coefficient corresponds to $\tilde{C}_{\rm b}=1$ (Table 1). The applied flow law is Nye–Glen with n=3.

We define three versions of the experiment. For all cases, to avoid the singularity associated with the binary switch between fully developed sliding and no-slip conditions, we allow for some exponentially decaying sub-melt sliding (e.g., Hindmarsh and Le Meur, 2001; Greve, 2005; Dunse and others, 2011) by setting $\tilde{C}_b \to \tilde{C}_b \exp(T_b'/\gamma_{\rm sms})$, where T_b' is the basal temperature relative to the pressure melting point (in °C, hence T_b' is non-positive), and $\gamma_{\rm sms}=3$ °C is the sub-melt-sliding parameter. Further, for all cases, we apply the dimensionless rate factor shown in Figure 1, which differs slightly from the original set-up. Experiment H1 employs linear Weertman sliding and the Nye–Glen flow law with n=3 as in the original set-up. For experiment H2, sliding has been changed to a Weertman–Budd law with (p,q)=(3,2) [no basal water pressure considered, $p_{b,w}=0$, cf. Eq. (2)], and for experiment H3, the stress exponent has been changed to n=4 (Table 2).

All experiments are carried out with SICOPOLIS v25. Ice dynamics is modelled by the depth-integrated viscosity approximation (DIVA) (Goldberg, 2011; Lipscomb and others, 2019; Grandadam, 2024), and for ice thermodynamics we employ the melting-CTS enthalpy method (CTS: cold-temperate transition surface) (Greve and Blatter, 2016). For the horizontal resolution, we use 10 km (rather than the 25 km from the original set-up), and we integrate over a model time of 100 ka starting from ice-free initial conditions, which is sufficient to reach a steady state for all three experiments.

Selected results (ice thickness, surface velocity, slip ratio = ratio of basal to surface velocity) are shown in Figure 2. Our main message is that all three experiments produce reasonable, consistent

Journal of Glaciology 5

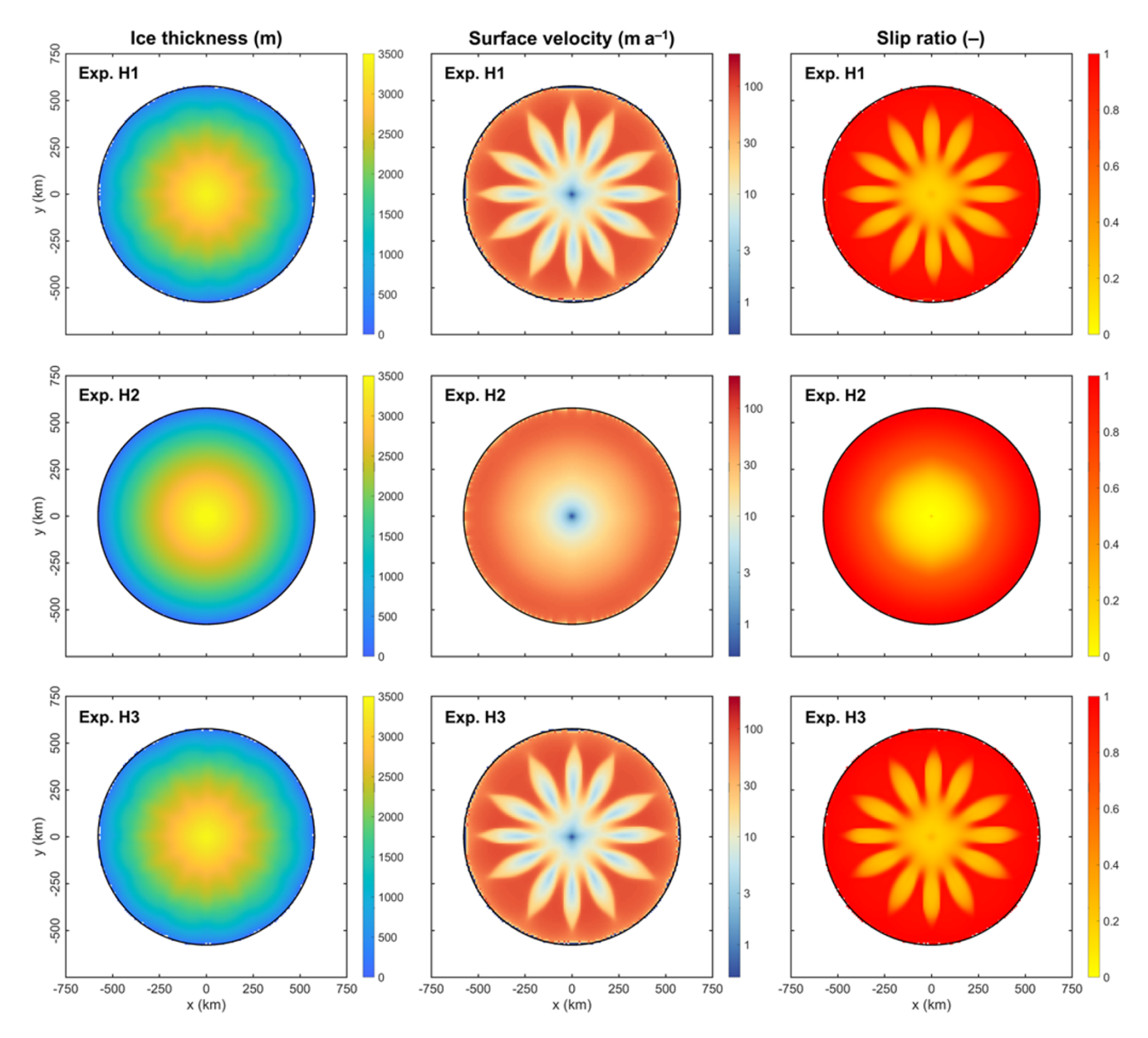


Figure 2. Simulated ice thickness, surface velocity and slip ratio (ratio of basal to surface velocity) for the three experiments (H1, H2, H3) described in the main text (Sect. 4) after 100 ka model time.

results for the same dimensionless sliding coefficient and rate factor, even though the exponents in the sliding law and the flow law have been varied. As explained above, in a dimensional formulation, this would require changes in the numerical values of the sliding coefficient and the rate factor by several orders of magnitude. The results of experiments H1 and H3 (flow-law exponent n changed) are very similar to each other and show a fingering instability that results from the thermomechanical coupling, which was already discussed in the original EISMINT publication by Payne and others 2000. By contrast, this instability does not occur in experiment H2 (sliding-law exponents p and q changed), where the solution maintains an almost perfect circular symmetry. While an interesting topic, we refrain from a deeper discussion of these instabilities here, yet point the interested reader to the EISMINT paper and further studies by, e.g., Fowler and Johnson (1996); Payne and Dongelmans (1997); Sayag and Tziperman (2008) and Hindmarsh 2009.

5. Summary

We presented non-dimensionalized forms of basal sliding laws and flow laws for use in dimensional ice-sheet and glacier models. Compared to their dimensional counterparts, these forms have the advantage that the coefficients (sliding coefficient, rate factor) become independent of the respective exponents. All of these parameters are to some extent uncertain and therefore candidates for systematic variation in ensemble simulations of ice sheets and glaciers, which becomes much easier with the dimensionless formulations as the parameters can be varied independently. This is particularly relevant for efforts to reproduce observations of the recent history of ice sheets and glaciers as a starting point for predictions of their future changes. As claimed, implementation in an existing dimensional ice-sheet model (SICOPOLIS v25) could be done with minimal adaptations. We demonstrated the practicability of the method by three test simulations for a simple,

6 Ralf Greve

idealized geometry, in which we varied the sliding-law exponents and the flow-law exponent while keeping the dimensionless sliding coefficient and rate factor constant.

Data availability statement. SICOPOLIS (SICOPOLIS Authors, 2025) is free and open-source software, published on a persistent Git repository hosted by GitHub (https://github.com/sicopolis/sicopolis/). The run-specs headers and output data produced for this study are available at Zenodo, https://doi.org/10.5281/zenodo.17373818.

Acknowledgements. The author thanks Ryszard Staroszczyk (Institute of Hydro-Engineering, Polish Academy of Sciences) and Shreyas Sunil Gaikwad (University of Texas at Austin, USA) for helpful discussions about flow laws and sliding laws, and Félix Grandadam (Claude Bernard University Lyon 1, France) for the implementation of DIVA in the SICOPOLIS model. The author further thanks the Associate Chief Editor Argha Banerjee, the Scientific Editor Ian Hewitt and two anonymous reviewers for their constructive remarks and suggestions.

Competing interests. The author serves as an Associate Chief Editor of the Journal of Glaciology.

References

- Bons PD and 6 others (2018) Greenland ice sheet: Higher nonlinearity of ice flow significantly reduces estimated basal motion. Geophysical Research Letters 45(13), 6542–6548. doi: 10.1029/2018GL078356
- Budd WF, Jenssen D and Smith IN (1984) A three-dimensional timedependent model of the West Antarctic ice sheet. Annals of Glaciology 5, 29–36. doi: 10.3189/1984AoG5-1-29-36
- Budd WF and Jenssen D (1987) Numerical modelling of the large-scale basal water flux under the West Antarctic ice sheet. In *Dynamics of the West Antarctic Ice Sheet*, CJ van der Veen and J Oerlemans (Eds.) D. Reidel Publishing Company, Dordrecht, The Netherlands pp. 293–320. doi: 10. 1007/978-94-009-3745-1
- Budd WF, Keage PL and Blundy NA (1979) Empirical studies of ice sliding. Journal of Glaciology 23(89), 157–170. doi: 10.3189/S002214300002 9804
- Cornford SL and 21 others (2020) Results of the third Marine Ice Sheet Model Intercomparison Project (MISMIP+). *The Cryosphere* 14(7), 2283–2301. doi: 10.5194/tc-14-2283-2020
- Cuffey KM and Paterson WSB (2010) The Physics of Glaciers, Amsterdam, The Netherlands etc: Elsevier. ISBN 978-0-12-369461-4
- Dunse T, Greve R, Schuler TV and Hagen JO (2011) Permanent fast flow versus cyclic surge behaviour: numerical simulations of the Austfonna ice cap, Svalbard. *Journal of Glaciology* 57(202), 247–259. doi: 10.3189/ 002214311796405979
- Fowler AC and Johnson C (1996) Ice-sheet surging and ice-stream formation. Annals of Glaciology 23, 68–73. doi: 10.3189/S0260305500013276
- Getraer B and Morlighem M (2025) Increasing the Glen-Nye power-law exponent accelerates ice-loss projections for the Amundsen Sea Embayment, West Antarctica. Geophysical Research Letters 52(7), e2024GL112516. doi: 10.1029/2024GL112516
- Glen JW (1955) The creep of polycrystalline ice. *Proceedings of the Royal Society* A 228(1175), 519–538. doi: 10.1098/rspa.1955.0066
- **Goldberg DN** (2011) A variationally derived, depth-integrated approximation to a higher-order glaciological flow model. *Journal of Glaciology* 57(201), 157–170. doi: 10.3189/002214311795306763
- Grandadam F (2024) Implementation of the Depth Integrated Viscosity Approximation in SICOPOLIS. Internship Report, Claude Bernard

- University Lyon 1, France, and Hokkaido University, Sapporo, Japan. doi: 10.5281/zenodo.14732938
- Greve R and Blatter H (2009) Dynamics of Ice Sheets and Glaciers, Berlin, Germany etc: Springer. ISBN 978-3-642-03414-5. doi: 10.1007/978-3-642-03415-2
- Greve R and Blatter H (2016) Comparison of thermodynamics solvers in the polythermal ice sheet model SICOPOLIS. *Polar Science* **10**(1), 11–23. doi: 10. 1016/j.polar.2015.12.004
- Greve R (2005) Relation of measured basal temperatures and the spatial distribution of the geothermal heat flux for the Greenland ice sheet. *Annals of Glaciology* 42, 424–432. doi: 10.3189/172756405781812510
- **Hindmarsh RCA** (2009) Consistent generation of ice-streams via thermoviscous instabilities modulated by membrane stresses. *Geophysical Research Letters* **36**(6), L06502. doi: 10.1029/2008GL036877
- **Hindmarsh RCA and Le Meur E** (2001) Dynamical processes involved in the retreat of marine ice sheets. *Journal of Glaciology* **47**(157), 271–282. doi: 10. 3189/172756501781832269
- Hooke RL (2005) Principles of Glacier Mechanics (2nd edition). Cambridge, UK and New York, NY, USA: Cambridge University Press. ISBN 9780511614231. doi: 10.1017/CBO9780511614231
- **Hutter K and Jöhnk K** (2004) *Continuum Methods of Physical Modeling*, Berlin, Germany: Springer. doi: 10.1007/978-3-662-06402-3
- **Lipscomb WH** and **14 others** (2019) Description and evaluation of the Community Ice Sheet Model (CISM) v2.1. *Geoscientific Model Development* **12**(1), 387–424. doi: 10.5194/gmd-12-387-2019
- Millstein JD, Minchew BM and Pegler SS (2022) Ice viscosity is more sensitive to stress than commonly assumed. *Communications Earth & Environment* 3. doi: 10.1038/s43247-022-00385-x
- Morlighem M, Seroussi H, Larour E and Rignot E (2013) Inversion of basal friction in Antarctica using exact and incomplete adjoints of a higher-order model. *Journal of Geophysical Research: Earth Surface* **118**(3), 1746–1753. doi: 10.1002/jgrf.20125
- Nye JF (1957) The distribution of stress and velocity in glaciers and ice sheets. Proceedings of the Royal Society A 239(1216), 113–133. doi: 10.1098/rspa. 1957.0026
- Payne AJ and Dongelmans PW (1997) Self-organization in the thermomechanical flow of ice sheets. *Journal of Geophysical Research: Solid Earth* 102(B6), 12219–12233. doi: 10.1029/97JB00513
- Payne AJ and 10 others (2000) Results from the EISMINT model intercomparison: the effects of thermomechanical coupling. *Journal of Glaciology* 46(153), 227–238. doi: 10.3189/172756500781832891
- **Rückamp M, Greve R and Humbert A** (2019) Comparative simulations of the evolution of the Greenland ice sheet under simplified Paris Agreement scenarios with the models SICOPOLIS and ISSM. *Polar Science* **21**, 14–25. doi: 10.1016/j.polar.2018.12.003
- Saito F, Abe-Ouchi A, Takahashi K and Blatter H (2016) SeaRISE experiments revisited: potential sources of spread in multi-model projections of the Greenland ice sheet. *The Cryosphere* 10(1), 43–63. doi: 10.5194/tc-10-43-2016
- Sayag R and Tziperman E (2008) Spontaneous generation of pure ice streams via flow instability: Role of longitudinal shear stresses and subglacial till. Journal of Geophysical Research: Solid Earth 113(B5), B05411. doi: 10.1029/2007IB005228
- Schohn CM, Iverson NR, Zoet LK, Fowler JR and Morgan-Witts N (2025) Linear-viscous flow of temperate ice. *Science* **387**(6730), 182–185. doi: 10. 1126/science.adp7708
- SICOPOLIS Authors (2025) SICOPOLIS v25. GitHub repository, GitHub. Available at https://github.com/sicopolis/sicopolis (accessed 30 June 2025).
- Weertman J (1957) On the sliding of glaciers. *Journal of Glaciology* 3(21), 33–38. doi: 10.3189/S0022143000024709